

## Deformability of Red Blood Cells : A Determinant of Blood Viscosity

**Sehyun Shin\*, Yunhee Ku, Myung-Su Park**

*School of Mechanical Engineering, Kyungpook National University,  
1370, Sankyuk-dong, Buk-gu, Daegu 702-701, Korea*

**Jang-Soo Suh**

*Department of Laboratory Medicine, Kyungpook National University Hospital,  
Daegu 700-721, Korea*

The suspension of hardened red blood cells (RBCs) differs from the suspension of normal RBCs with respect to their rheological behavior. The present study investigated the effect of deformability of RBCs on blood viscosity. RBC deformability and blood viscosity were measured with a recently developed slit-flow laser-diffractometer and the pressure-scanning capillary viscometer, respectively. At the same level of cell concentration, the viscosity of the hardened RBC suspension is higher than that of the normal RBCs suspension. An increase in cell percentage for hardened RBCs shows the significant increase in the level of blood viscosity compared to the normal RBCs. In addition, it was found that RBC deformability played an important role in reducing viscosity at low shear rates as well as high shear rates. These results present the evidence for the effect of RBC deformability on blood viscosity using newly developed methods, which can be used in early diagnosis of the cardiovascular diseases.

**Key Words :** RBC ; Deformability ; Viscosity ; Blood ; Diagnosis

### Nomenclature

EI : elongation index  
 h : slit gap, [m]  
 L : slit length, [m]  
 n : number of samples  
 P : pressure, [kPa]  
 $\Delta P$  : pressure difference ( $=P_A - P$ )  
 Q : volume flow rate, [m<sup>3</sup>/s]  
 V : volume, [m<sup>3</sup>]  
 t : time, [s]  
 w : slit width, [m]  
 X : length of major axis of ellipse  
 Y : length of minor axis of ellipse

### Greek Symbols

$\rho$  : density, [kg/m<sup>3</sup>]  
 $\eta$  : non-Newtonian viscosity, [Pa·s]  
 $\dot{\gamma}$  : shear rate, [s<sup>-1</sup>]  
 $\tau$  : shear stress, [Pa]

### Subscripts

A : atmosphere  
 avg : averaged  
 w : wall

## 1. Introduction

Red blood cells (RBCs) are highly specialized cells that carry oxygen from the lungs to the tissue and allow carbon dioxide to move from the tissue to the lungs. RBCs are biconcave disks of 8  $\mu\text{m}$  in diameter and 2  $\mu\text{m}$  thick as shown in Fig. 1. The unique shape and structure of RBC confer special mechanical properties to the cells (Chien, 1987; Mohandas and Chasis, 1993). Normal

---

\* Corresponding Author,

E-mail : shins@wmail.knu.ac.kr

TEL : +82-53-950-6570; FAX : +82-53-954-5034

School of Mechanical Engineering, Kyungpook National University, 1370, Sankyuk-dong, Buk-gu, Daegu 702-701, Korea. (Manuscript Received July 7, 2004; Revised April 12, 2004)

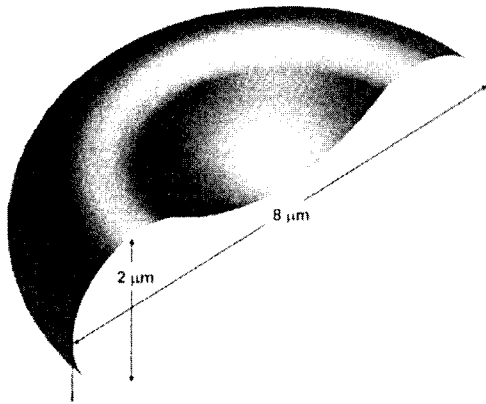


**Fig. 1** Red blood cell structure

RBCs readily deform with extensive changes in their shape when subjected to shear stress. The degree of deformation under a given force is defined as RBC deformability.

In fact, RBCs behave as elastic bodies and thus the deformation is reversible when the applied force is removed (Evans and LaCelle, 1975). RBCs also exhibit viscous behavior and thus respond as a viscoelastic body. Like shock absorbers on cars, the force needed to deform a RBC increases with both the extent and the rate of deformation. In addition, the RBC membrane can exhibit plastic changes under some pathological circumstances and can become deformed permanently by excessive shear forces. These characteristics of RBCs come from the RBC membrane and its underlying cytoskeleton. The lipid bilayer of the membrane is purely viscous and makes almost no contribution to the elastic behavior of the RBC membrane. Rather, it is now generally accepted that the RBC membrane cytoskeleton is mainly responsible for the maintenance of the biconcave-discoid shape (Hochmuth and Waugh, 1986). The RBC membrane cytoskeleton is a network of proteins which lie just beneath the cell membrane and the protein spectrin is known to be the most important component of this network (Lux, 1979).

The deformability of RBCs plays a key role in blood circulation since they have to pass through capillaries whose diameter is smaller than their size. This RBC deformability is also known to be

responsible for the surprisingly low viscosity at high shear rates in the large arteries, although whole blood consists of almost 50% of the volume of the blood cells (Chien, 1987). A slight decrease in red cell deformability may reduce the rate of entry into the capillaries and subsequently cause serious diseases such as diabetes (Diamantopoulos et al., 2004), hypertension (Puniyani et al., 1992), sickle cells (Hiruma et al., 1995) and myocardial infarction. A large variety of diseases have been described in association with less deformable RBCs (Lowe et al., 1988). Thus, the objective of this paper was to investigate the effect of the deformability on blood viscosity.

Meanwhile, various techniques in measuring the deformability of RBCs have been proposed and their comparison can be found elsewhere (Stoltz et al., 1999; Wang et al., 1999). Typical techniques can be briefly summarized as follows: (i) *RBC filtration*: This method has been widely used in measuring RBC deformability due to its similarity and simplicity (Hanss, 1983). Deformability can be determined by measuring either the pressure built up across the membrane during a test period or the transit time related to a certain number of RBCs. There, however, is a major drawback to this method in that a calibration standard is lacking; (ii) *Rheoscope* (Dobbe et al., 2002 & 2004; Guck et al., 2001): It is a direct observation of the shape of RBCs under given shear stress level. Other methods such as centrifugation and micropipette aspiration were also used to measure RBC deformability; (iii) *Ektacytometry* (Hardeman et al., 1994, Wang et al., 1999): The principle of this technique uses laser diffraction analysis of RBCs under varying stress levels, which was developed after the work of Bessis and Mohandas (1975). The advantage of this technique is that the cellular deformability of a number of cells can be measured rapidly using extremely small quantities of blood (less than 50 μl). The Extacytometer has been further developed and is commercially available by companies such as LORCA® (R&R Mechatronics, Hoorn, Netherlands) and RHEODYN SSD (Myrenne, Roetgen, Germany).

Although there are many methods and instru-

ments for measuring deformability as described above, most of the current techniques including ektacytometry require cleaning after each measurement. In order to measure cell deformability in a clinical setting, one needs to repeat the cleaning process after each measurement. This leads to a labor-intensive and time-consuming process. Hence, the current techniques are not optimal for day-to-day clinical use. The preliminary study introduced a new laser-diffraction slit rheometer (LDSR) as proof of the principle (Shin et al., 2004a). Since this device adopted a disposable element which is in contact with the blood samples, it can be used in a clinical setting. Thus, the objective of the present study is to examine the effect of RBC deformability on blood viscosity using newly developed methods, which can be easily used in clinical settings due to incorporating disposable elements that holds the blood sample. In the present study, the LDSR was further developed with modifications, which was used as the main instrument to measure RBC deformability for normal and artificially hardened cells.

## 2. Materials and Methods

### 2.1 Sample preparation

Blood was obtained from six normal, healthy volunteers who were not on any medications and who provided informed consent (age range 25–40

years and male/female participants). The blood samples used in the experiments were not pooled from more than one individual subject and all analyses were completed within six hours after blood collection. The samples of venous blood were drawn from the antecubital vein and collected in an EDTA containing Vacutainers (BD, Franklin Lakes, NJ).

Then, the RBCs were separated from the whole blood by centrifugation 1,200 g for 10 min. and washed with a 1 mM phosphate buffered saline (PBS; pH=7.4; osmolarity 290 mOsm/kg). In order to make hardened RBCs, the washed RBCs were exposed to a solution of hydrogen peroxide ( $H_2O_2$ , Green Pharm Co., Ltd, Korea) with a concentration level (2 mM) at 25°C for 30 min. Following the treatment with the control period, the RBCs were rewashed in a PBS and resuspended in a 5.5% PVP solution in a PBS at the optimal hematocrit, which were used for deformability by the present slit diffractometer. In order to check the reproducibility of the present LDSR, 10 measurements were carried out with the same normal blood sample. Blood samples were divided into two groups: (i) normal RBCs ( $n=5$ ); and (ii) RBCs exposed to  $H_2O_2$  at levels of 2 mM for 30 minutes ( $n=5$ ).

### 2.2 Apparatus and operation

The basic apparatus of the LDSR, containing a laser, CCD video camera, screen, and pressure

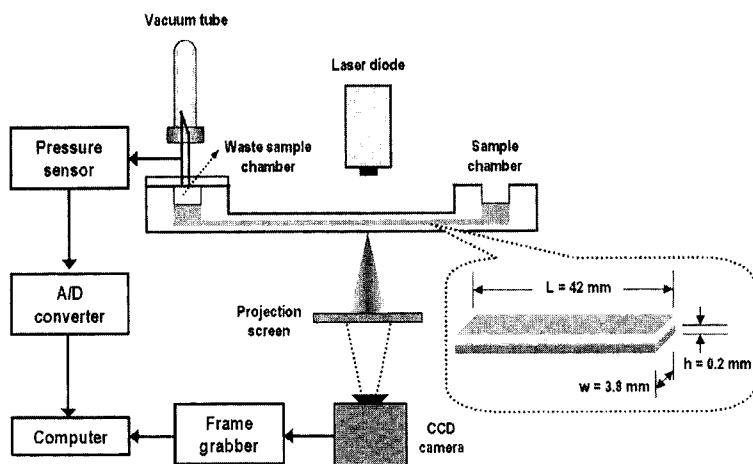


Fig. 2 Schematic diagram of a laser-diffraction slit rheometer

driven slit rheometry, is shown in Fig. 2. The laboratory setup also consisted of a computer. Details of the pressure-driven slit rheometry can be found elsewhere (Shin et al., 2004b), which consists of a vacuum tube, disposable test slit with two chambers, pressure transducer and a computer data acquisition system. The blood sample is sheared in the slit channel with a gap of 0.2 mm, a width of 3.8 mm and a length of 42.3 mm. The slit which is integrated with two chambers is disposable, and is made of transparent polystyrene using micro-injection molding. The diode laser (635 nm, 1.5 mW) and a CCD camera (SONY-ES30) combined with a frame grabber were used to obtain a laser-diffraction pattern. The diffraction pattern is analyzed by an ellipse-fitting-program and the elongation indices ( $EI$ ) are calculated for shear stress levels between 0~20 Pa. The length and gap of the slit were chosen to ensure that the friction loss in the slit was the dominant loss in the system.

Typical tests are conducted as follows : When the preset vacuum chamber is pushed into the connecting needle, the vacuum pressure rapidly moves towards to the waste sample chamber tube, which drives the test fluid to flow through the slit by the differential pressure between the two chambers. As the waste sample chamber is being filled with the incoming fluid, the differential pressure is gradually released. When the differential pressure reaches an equilibrium, the test fluid stops flowing.

While the test blood flows through the slit, a laser beam emitting from the laser diode traverses the diluted RBC suspension and is diffracted by the RBCs in the volume. The diffraction pattern projected onto the screen is captured by the CCD-video camera, which is linked to the frame grabber integrated with a computer. While the differential pressure decreases, the shape of the RBCs changes gradually from a prolate ellipsoid towards a biconcave circular morphology. The Elongation Index ( $EI$ ), as a measure of RBC deformability, is determined from an isointensity curve in the diffraction pattern using an ellipse-fitting program. In order to confirm the reliability of the present method, the elongation index of the

diluted RBCs was also measured by the commercial rotating type ektacytometry, LORCA (R&R Mechatronics, Netherlands) and these results compared with the results of the present slit-flow ektacytometry.

The essential feature of the LDSR was the simultaneous measuring of pressure and diffraction patterns. A precision pressure transducer (Validyne, DP15) was used to measure the pressure difference between the vacuum chamber and atmosphere,  $\Delta P(t)$ , every 0.5s with a resolution of 1 Pa. From the measured pressure difference, the corresponding wall-shear stress can be determined from the following equation (Shin et al., 2004b).

$$\tau_w(t) = \frac{\Delta P(t) h/L}{(1+2h/w)} \quad (1)$$

It is worthy to note that in the present slit diffractometer the optical measurement of the diffraction pattern reflects the elongation of cells at all depths in the pressure-driven slit flow, and hence the elongation of cells which experience shear stress levels from zero up to the wall shear stress. Thus, the present study introduced an average shear stress level as a characteristic shear stress, which is defined as

$$\tau_{avg} = \frac{2}{h} \int_0^{\frac{1}{2}h} \tau(y) dy. \quad (2)$$

Since the shear stress profile in a fully developed slit flow is a linear function of  $y$  as shown in Eq. (1), the average shear stress amounts to one-half of the wall shear stress ( $\tau_{avg} = 1/2 \tau_w$ ).

A detailed description of the stress-shear rate relation can be found in a previous study (Shin et al., 2002 and 2004b). A brief description is as follows : In deriving the stress-shear rate relation in the capillary viscometer, the important assumptions are 1) a fully developed, isothermal, laminar flow ; 2) no slip at the walls ; and 3) air in the vacuum chamber as an ideal gas. On the assumption that the product of pressure  $P(t)$  and volume  $V(t)$  in the vacuum chamber at time  $t$  is constant,  $P_i V_i = P(t) V(t)$ , where subscript  $i$  represents the initial state of the experiment, the instantaneous pressure  $P(t)$  is recorded in the

computer file. The flow rate at time  $t$  can be obtained by  $Q(t) = \frac{d}{dt} \left( \frac{P_i V_i}{P(t)} \right)$ . On the other hand, the pressure difference through a slit can be expressed as  $\Delta P = \{ P_A - P(t) \}$  and the corresponding shear stress is determined from Eq. (1). Further mathematical equations including the shear rate and viscosity can be found elsewhere (Shin et al., 2004b; Macosco, 1994). For the viscosity measurement of various RBC suspensions, we used the pressure-scanning capillary viscometer (PSCV), which was developed for our previous study (Shin et al., 2002).

### 3. Results and Discussion

Figure 3 shows variations of the average shear stress and diffraction patterns over time for a RBC suspension. As shown in Fig. 3, the shear stress decreases exponentially over time since the pressure differential decreases as the waste sample chamber is being filled with the incoming fluid. In addition, the instantaneous diffraction patterns gradually change from a prolate ellipsoid shape to the original circular shape. The Elongation Index ( $EI$ ), as a measure of RBC deformability, is determined from an isointensity curve in the diffraction pattern using an ellipse-fitting program. The  $EI$  is defined as  $(X - Y)/(X + Y)$ , where  $X$  and  $Y$  are the major and minor axes of the ellipse, respectively. Typically, it took approximately 1~2 min to complete a test as shown in Fig. 3.

Figure 4 compares the mean values of  $EI$  for normal erythrocytes measured with the present LDSR and LORCA as a function of the applied shear stress. The rectangles indicate the  $EI$  measured with the LORCA, and circles indicate those measured with the LDSR. Compared with these results, the test results provide a good correlation between two instruments with less than a 2.3% error rate across the entire shear stress range.

Meanwhile, the present study measured RBC deformability with the present LDSR. In order to vary the deformability of the RBCs, they were hardened by incubating in a solution of hydrogen peroxide. It has been known that the higher the

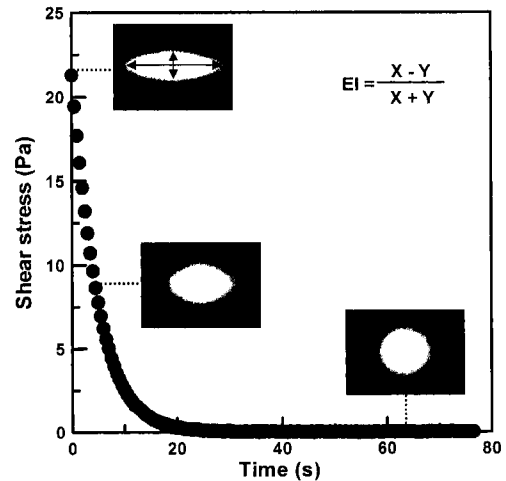


Fig. 3 Variations of shear stress and diffraction pattern along time

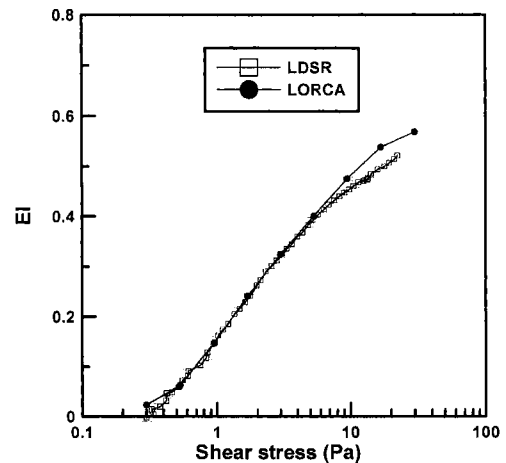


Fig. 4 Comparison of  $EI$  values for control blood between LDSR and LORCA

level of concentration used, the less deformable the RBCs become. Figure 5 shows the Elongation Index ( $EI$ ) over a range of shear stress for normal RBCs, hardened RBCs and solid particles (Zeolite, Sigma, USA). The normal RBCs show the highest plateau value of  $EI$  at a high shear stress. The artificially hardened RBCs show lower values of  $EI$  than the normal blood. In addition the  $EI$  values for the solid particles does not varies over a range of shear stress.

Meanwhile, after measuring the deformability for RBCs and particles, the corresponding vis-

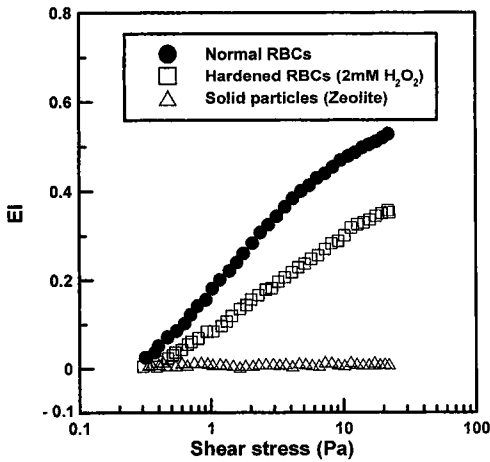


Fig. 5 Elongation Index versus shear stress for normal RBCs, hardened RBCs and solid particles

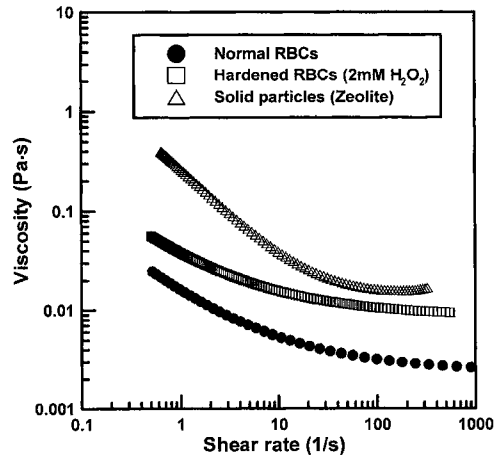


Fig. 7 Suspension viscosity versus shear rate for normal RBCs, hardened RBCs and solid particles

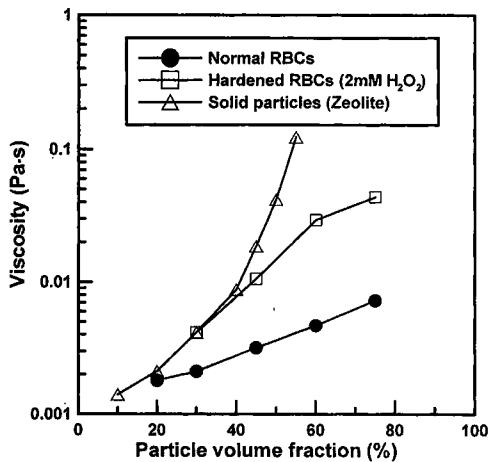


Fig. 6 High shear viscosity versus volume fraction for normal RBCs, hardened RBCs and solid particles

cosity was measured by the pressure-scanning capillary viscometer (PSCV). Figure 6 shows viscosity at high shear rate ( $\dot{\gamma} > 100s^{-1}$ ) for three different suspensions along particle volume fractions. This figure demonstrates the amazing fluidity of normal blood compared with that of other suspensions. At 45% concentration, the suspension viscosity of the hardened cells (exposed to 2 mM  $H_2O_2$ ) is so high that it would be expected to cause cardiovascular diseases such as retinopathy and cerebral ischemia (Testa et al., 1995). In addition, the suspension viscosity of the solid

particles increases exponentially with the particle volume fraction, which has been well known (Jeffrey and Acrivos, 1977). The normal blood viscosity, however, shows a relatively low value even at high volume fractions. Thus, these results imply that the RBCs, which have less deformability such as deoxygenated sickle cells, may be the cause of a serious circulation disease, which is called sickle cell anemia (Diamantopoulos et al., 2004).

Figure 7 shows RBC suspension viscosity along shear rate for various particles which have a different level of deformability at a fixed particle volume fraction of 0.45. All viscosity curves of the suspensions show a shear-thinning characteristic, which is mainly due to disaggregation of the RBCs or particles in the suspending media with increasing shear rate. It is observed that the more hardened the particles are, the higher the suspension viscosity becomes. In addition, RBC deformability affects not only high-shear viscosity but also low-shear viscosity. In fact, it has been known that deformability affects mainly the high shear viscosity of blood, so that the high shear viscosity at a low cell volume fraction has been used as an indirect measurement of RBC deformability (Chien et al., 1967). This, however, may not be true at a high cell volume fraction such as a physiological condition ( $H=0.45$ ), since there are various possibilities for RBC aggregation

depending on its deformability. Recently, Baskurt and Meiselman (2003) also confirmed that the RBC aggregation is also affected by cellular properties including RBC deformability. Thus, it may be interesting to further consider the deformability-dependent blood viscosity with RBC aggregation, shearing conditions, and cell volume fraction.

#### 4. Conclusion

The deformability of normal and hardened RBCs and their suspension viscosity were measured with LDSR and PSCV, respectively. The results which were taken with the present LDSR showed a correlation with those of a commercial ektacytometer (LORCA). RBC deformability was found to be the major determinant of the blood viscosity over a range of shear rates and its physiological importance was demonstrated in the present study. Thus, if RBC deformability and blood viscosity measurements are included in routine blood tests, they would provide very meaningful information with other chemical analysis data, such as a cholesterol level.

#### Acknowledgments

This work was supported by a Grant from the National Research Laboratory of the Ministry of Science and Technology, Korea.

#### References

- Baskurt, O. K. and Meiselman, H. J., 2003, "Blood Rheology and Hemodynamics," *Seminars in Thrombosis and Hemostasis*, Vol. 29, pp. 435.
- Bessis, M. and Mohandas, N., 1975, "A Differential Method for the Measurement of Cellular Deformability," *Blood Cells*, Vol. 1, pp. 307~312.
- Chien, S., Usami, S., Dellenback, R. J. and Gregersen, M.I., 1967, "Blood Viscosity: Influence of Erythrocyte Deformation," *Science*, Vol. 157, pp. 827~829.
- Chien, S., 1987, "Red Cell Deformability and its Relevance to Blood Flow," *Annu Rev Physiol.*, Vol. 49, pp. 177~192.
- Diamantopoulos, E. J., Kittas, C., Charitos, D., Grigoriadou, M., Ifanti, G. and Raptis, S. A., 2004, "Impaired Erythrocyte Deformability Precedes Vascular Changes in Experimental Diabetes Mellitus," *Horm. Metab. Res.* Vol. 36, pp. 142~147.
- Dobbe, J. G. G., Hardeman, M. R., Streekstra, G. J., Strackee, J., Ince, C. and Grimbergen, C. A., 2002, "Analyzing Red Blood Cell-Deformability Distributions," *Blood Cells, Molecules, and Diseases*, Vol. 28, pp. 373~384.
- Dobbe, J. G. G., Hardeman, M. R., Streekstra, G. J., Strackee, C. and Grimbergen, C. A., 2004, "Validation and Application of an Automated Rheoscope for Measuring Red Blood Cell Deformability Distributions in Different Species," *Biorheology*, Vol. 41, pp. 65~77.
- Evans, E. A. and LaCelle, P. L., 1975, "Intrinsic Material Properties of Erythrocyte Membrane Indicated by Mechanical Analysis of Deformation," *Blood*, Vol. 45, pp. 29~43.
- Guck, J., Ananthakrishnan, R. Mahmood, Moon, T. J., Cunningham, C. C. and Ka, J., 2001, "The Optical Stretcher: A Novel Laser Tool to Micromanipulate Cells," *Biophysical J.*, Vol. 81, pp. 767~784.
- Hanss, M., 1983, "Erythrocyte Filterability Measurement by the Initial Flow Rate Method," *Biorheology*, Vol. 20, pp. 199~211.
- Hardeman, M. R., Goedhart, P. T., Dobbe, J. G. G. and Lettinga, K. P., 1994, "Laser-assisted Optical Rotational Cell Analyser (LORCA): A New Instrument for Measurement of Various Structural Hemorheological Parameters," *Clin. Hemorheol.* Vol. 14, pp. 605~610.
- Hiruma, H., Noguchi, C. T., Uyesaka, N., Schechter, A. N. and Rodgers, G. P., 1995, "Contributions of Sick Cell Hemoglobin Polymer and Sick Cell Membranes to Impaired Filterability," *Am. J. Physiol.*, Vol. 268, pp. H2003~2008.
- Hochmuth, R. M. and Waugh, R., 1986, "Erythrocyte Membrane Elasticity and Viscosity," *Annu Rev Physiol.*, Vol. 49, pp. 209~219.
- Jeffrey, D. J. and Acrivos, A., 1977, "The Rheological Properties of Suspensions of Rigid Particles," *AIChE J.* Vol. 22, pp. 417~432.

- Lowe, G., 1988. *Clinical Blood Rheology*, CRC Press, Boca Raton, FL.
- Lux, S. E., 1979, "Dissecting the Red Cell Membrane Skeleton," *Nature*, Vol. 281, pp. 426~429.
- Macosko, C. W. 1993, *Rheology : Principles, Measurements, and Applications*, VCH, New York, pp. 237~258.
- Mohandas, N. and Chasis, J. A., 1993, "Red Blood Cell Deformability, Membrane Material Properties and Shape: Regulation by Transmembrane, Skeletal and Cytosolic Proteins and Lipids," *Semin Hematol.*, Vol. 30, pp. 171~192.
- Puniyani, R. R., Ajmani, R. and Kale, P. A., 1991, "Risk Factors Evaluation in Some Cardiovascular Diseases," *J. Biomed. Eng.*, Vol. 13, pp. 441~443.
- Shin, S., Keum, D. Y. and Ku, Y. H., 2002. "Blood Viscosity Measurement Using a Pressure-Scanning Capillary Viscometer," *KSME Int. J.*, Vol. 16, pp. 1719~1724.
- Shin, S., Ku, Y. H., Park, M. S. Moon, S. Y., Jang, J. H. and Suh, J. S., 2004a, "Laser-diffraction Slit Rheometer to Measure Red Blood Cell Deformability," *Rev. Sci. Instr.*, Vol. 75, pp. 559~561.
- Shin, S., Lee, S. W. and Ku, Y. H., 2004b, "Measurements of Blood Viscosity using a Pressure-scanning Slit Viscometer," *KSME Int. J.*, Vol. 18, pp. 1036~1041.
- Stoltz, J. -F., Singh, M. and Riha, P., 1999, *Hemorheology in Practice*, IOS Press, Amsterdam, Netherlands, pp. 67~72.
- Testa, I., Manfrini, S., Gregorio, F., Refe, A., Bonfigli. A. R., Testa, R. and Piantanelli, L., 1995, "Red Blood Cell Deformability in Diabetic Retinopathy," *Biorheology*, Vol. 32, pp. 389~395.
- Wang, X., Zhao, H., Zhuang, F. Y. and Stoltz, J. F., 1999, "Measurement of Erythrocyte Deformability By two Laser Diffraction Methods," *Clinical Hemorheol. and Microcirculation*, Vol. 21, pp. 291~295.